Regular Articles

Nicotine-Induced Limbic Cortical Activation in the Human Brain: A Functional MRI Study

Elliot A. Stein, Ph.D., John Pankiewicz, M.D., Harold H. Harsch, M.D., Jung-Ki Cho, M.D., Scott A. Fuller, B.S., Raymond G. Hoffmann, Ph.D., Marjorie Hawkins, M.D., Stephen M. Rao, Ph.D., Peter A. Bandettini, Ph.D., and Alan S. Bloom, Ph.D.

Objective: Nicotine is a highly addictive substance, and cigarette smoking is a major cause of premature death among humans. Little is known about the neuropharmacology and sites of action of nicotine in the human brain. Such knowledge might help in the development of new behavioral and pharmacological therapies to aid in treating nicotine dependence and to improve smoking cessation success rates. **Method:** Functional magnetic resonance imaging, a real-time imaging technique, was used to determine the acute CNS effects of intravenous nicotine in 16 active cigarette smokers. An injection of saline followed by injections of three doses of nicotine (0.75, 1.50, and 2.25 mg/70 kg of weight) were each administered intravenously over 1-minute periods in an ascending, cumulative-dosing paradigm while whole brain gradient-echo, echo-planar images were acquired every 6 seconds during consecutive 20-minute trials. **Results:** Nicotine induced a dose-dependent increase in several behavioral parameters, including feelings of "rush" and "high" and drug liking. Nicotine also induced a dose-dependent increase in neuronal activity in a distributed system of brain regions, including the nucleus accumbens, amygdala, cingulate, and frontal lobes. Activation in these structures is consistent with nicotine's behavior-arousing and behavior-reinforcing properties in humans. **Conclusions:** The identified brain regions have been previously shown to participate in the reinforcing, mood-elevating, and cognitive properties of other abused drugs such as cocaine, amphetamine, and opiates, suggesting that nicotine acts similarly in the human brain to produce its reinforcing and dependence properties.

(Am J Psychiatry 1998; 155:1009–1015)

Tobacco dependence is the most common substance abuse disorder and the leading preventable cause of death in the United States (1). It meets all of the DSM-IV criteria for drug dependence, including compulsive use, difficulty in quitting, and withdrawal symptoms upon cessation of chronic use. Only about 3% of smokers who try to quit remain abstinent for 1 year (2). Although there are more than 2,000 compounds in cigarette smoke, nicotine alone has been shown to produce tolerance, dependence, and a distinct withdrawal syndrome in both animals and humans (3). It is generally considered to be the addictive and reinforcing agent responsible for continued smoking behavior (1, 4, 5), and while the mechanisms underlying its reinforcing properties are not well understood, nicotine is thought to interact with the mesocorticolimbic dopamine system in a manner similar to that of other abused drugs such as cocaine (3, 6, 7).

Nicotine produces profound behavioral effects in hu-

Data presented in part at the College on Problems of Drug Dependence, Scottsdale, Ariz., June 10–15, 1995. Received Sept. 22, 1997; revision received March 23, 1998; accepted April 3, 1998. From the Departments of Psychiatry, Pharmacology, Neurology, and Biostatistics and the Biophysics Research Institute, Medical College of Wisconsin. Address reprint requests to Dr. Stein, Department of Psychiatry, Medical College of Wisconsin, 8701 Watertown Plank Rd., Milwaukee, WI 53226; estein@mcw.edu (e-mail).

Supported in part by grant DA-09465 from the National Institute on Drug Abuse to Dr. Stein and NIH General Clinical Research Center grant RR-00058.

FIGURE 1. Mean Serum Nicotine Concentrations, as Determined by Gas Chromatography-Mass Spectrometry, of 16 Subjects After Three Different Intravenous Doses of Nicotine[a]

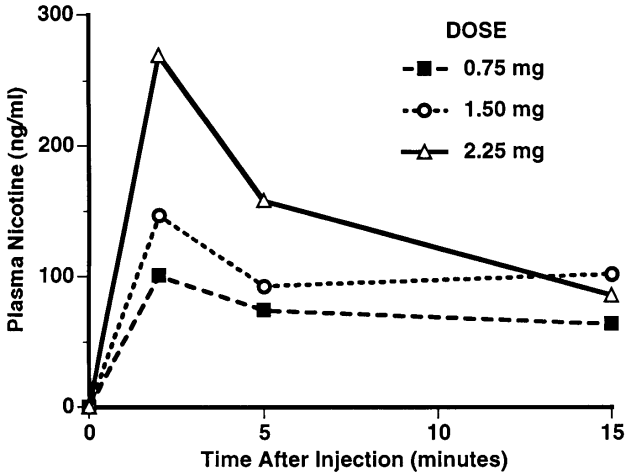

[a]Analysis of variance indicated a significant effect of time ($F=4.11$, $df=2, 46$, $p\leq0.02$) and dose ($F=4.50$, $df=2, 46$, $p\leq0.02$). There was no time-by-dose interaction, indicating that the serum half-lives among the doses were not significantly different.

mans, including memory facilitation, locomotor activation, mild anti-nociception, calming, and appetite suppression (8). However, little is known of nicotine's effects on neuronal activity at a systems level in animals (9–11), and almost nothing is known about this in humans. Understanding the sites and mechanisms of nicotine's action in the human brain, along with our knowledge of its behavioral pharmacology and its potential addictive properties in common with those of other abused substances, may lead to new concepts related to the central mechanisms of drug dependence and the development of novel smoking cessation therapies.

Functional magnetic resonance imaging (MRI) allows for the noninvasive study of human brain activity by measuring localized, intrinsic signal changes that are directly driven by changes in neuronal activity. Because of its excellent temporal and spatial resolution, we used this imaging tool to identify neuroanatomical regions activated by nicotine in the human brain. We hypothesized that frontal lobe and limbic/cingulate cortical structures would be activated by nicotine, consistent with the drug's mood-altering, attentional, and vigilance properties. Further, since nicotine is a stimulant and addictive agent, we hypothesized that regions previously implicated in animal models of drug abuse, such as the nucleus accumbens, would also be activated in humans after nicotine administration.

METHOD

Subjects were recruited through newspaper advertisements. They were generally healthy individuals (nine male and seven female) between the ages of 18 and 39 years (mean=25.9, SD=6.0) with smoking histories averaging 8.5 years (SD=5.4, range=1.5–23) and current use of about one pack of cigarettes per day. All but two subjects were strongly right-handed according to the Edinburgh Handedness Inventory (12). The subjects had no previous history of any neurological or psychiatric disorder and no other drug dependence. The experiments were approved by the institutional review board of the Medical College of Wisconsin. Brief physical and history examinations were conducted before the initiation of any experimental procedure. After complete description of the study to the subjects, written informed consent was obtained. Subjects were instructed that they should smoke as they wished during all phases of their participation in the study. Their only restriction was no alcohol consumption for 24 hours and no caffeine consumption for 12 hours before scanning.

To determine safety and obtain physiological and behavioral measures, before their scanning session the subjects received an intravenous injection of saline into an antecubital vein, followed by three injections of nicotine (0.75, 1.50, and 2.25 mg/70 kg of body weight). All injections lasted for 1 minute and occurred in ascending dose order every 20–30 minutes while the subjects were recumbent in bed at the Medical College of Wisconsin General Clinical Research Center. Subjects were continuously monitored for blood pressure and pulse rate and by ECG and were asked to respond on 10-point Likert scales at 2, 5, and 15 minutes after injection to eight behavioral rating questions (feelings of "rush," "high," pleasantness, anxiety, confusion, and sedation, intensity of drug effect, and drug liking). A second intravenous catheter was used to collect blood samples for determination of serum nicotine concentrations by gas chromatography-mass spectrometry (13).

Approximately 1 week later, the same three doses of nicotine were administered while the subjects underwent functional MRI scanning. The subjects reported to the MRI facility approximately 30 minutes before their scan appointment. All of them reported smoking a cigarette immediately before entering the hospital. Scan sessions, approximately 2 hours in duration, began between 8:00 p.m. and 1:00 a.m.

Whole brain functional MRI data were acquired with a 1.5-T Signa scanner (GE Medical Systems, Milwaukee) equipped with a 30.5-cm internal diameter three-axis, balanced-torque local gradient coil designed specifically for rapid gradient switching and a shielded-quadrature elliptical encapped transmit/receive birdcage radio frequency coil inserted inside the gradient coil (14). Eight contiguous 8-mm axial slices were acquired with use of a blipped, gradient-echo, echo-planar image pulse sequence (TE=40 msec) with an interscan resolution of 6 seconds during the 20-minute acquisition period and a 24-cm field of view with an in-plane resolution of 3.75 mm. During each 20-minute scan, the first 4 minutes consisted of baseline data acquisition, followed by the 1-minute intravenous injection, and then 15 minutes of postdrug data acquisition. The blood-oxygen-level-dependent pulse sequence we used is weighted to be most sensitive to changes in blood oxygenation levels rather than blood flow alterations. Anatomical images (spoiled gradient/recall acquisition in the steady state [GRASS], 256×256 pixels, 1.1 mm thick) were acquired immediately before functional MRI data acquisition.

Functional MRI data were analyzed with an algorithm and associated software that we developed, which is based on the working hypothesis that parenchyma-derived signals should follow a pharmacokinetic model; that is, the arterial drug concentration curve is posited to reflect the brain drug concentration distribution, which in turn drives brain activation patterns (A.S. Bloom et al., manuscript submitted for publication). Active voxels were detected according to six criteria: time to peak effect (1–8 minutes after the start of the injection), magnitude and statistical significance of the peak effect ($\geq0.5\%$ over baseline and $p\leq10^{-6}$, unpaired t test), slope of the rising phase of the response curve (0.5–5.0), time to decline back to 50% of the peak effect (4–12 minutes after injection), and baseline period stability ($\leq11\%$ of the mean range for all voxels in the brain). The acceptable range given in parentheses for each parameter was determined from the known pharmacokinetics of nicotine, the observed venous blood levels, and the physiological and behavioral effects seen in this study. To be considered active, a voxel had to meet all of the six criteria. Functional images were generated by applying the algorithm to each pixel and overlaying activated regions on high-resolution, three-dimensional spoiled GRASS images. Nearest-neighbor pixel analysis was performed to preclude isolated pixel recognition. All data were transformed into the stereotaxic coordinate system of

FIGURE 2. Functional MRI Time Course Data on a Single Subject After Intravenous Injection of 1.50 mg of Nicotine[a]

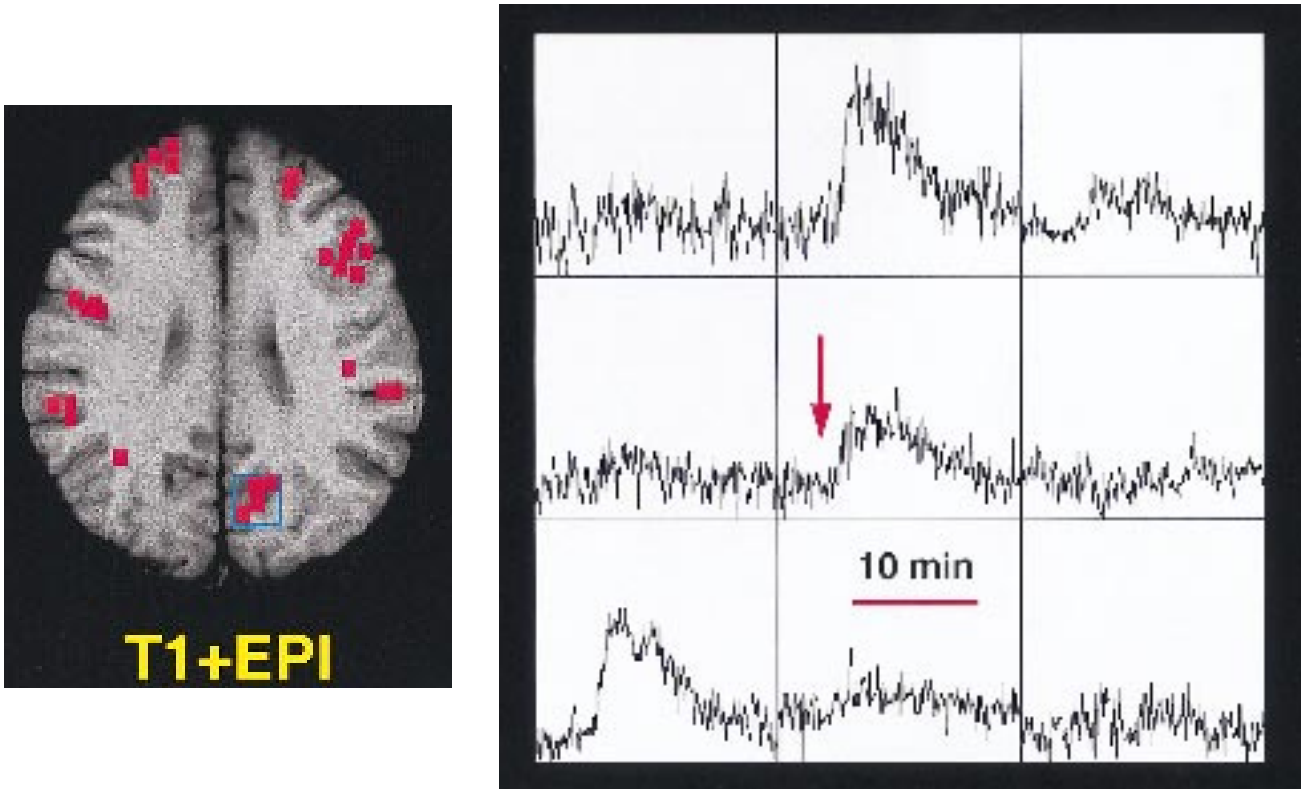

[a]Superimposed on the T_1-weighted, fast spin echo-planar image (EPI) is a map of all nicotine-activated voxels (red boxes) from that brain slice (left side). The box outlined in blue denotes the 3×3 voxel region of interest corresponding to the time course data shown on the right side of the figure. The nine independent time course graphs (right side) illustrate the functional MRI signal plotted against time and are derived from the nine contiguous voxels depicted in the posterior cingulate. The arrow indicates the onset time of the 1-minute injection. Note the rapid rise in signal in three of the voxels and its exponential time decay, with the signal returning to baseline within 15 minutes. These three voxels, plus the smaller effect seen in the upper right voxel, were among those that both met the criteria of the waveform recognition algorithm and were indicated within the region-of-interest box. Note also the heterogeneous nature of the response, with adjacent 3.75-mm voxels showing no apparent drug effect.

Talairach and Tournoux (15), averaged across all subjects at each dose to produce mean dose-response activation maps, and displayed with the use of AFNI (16). To compensate for the anatomical uncertainty of the Talairach and Tournoux transformation, a 3-mm blur was formed around activated pixels.

Statistical significance for the combined group data was determined on the basis of a probability function derived from a beta binomial distribution of each individual's response after the saline injection. A centers-of-mass analysis was used to determine regions of interest, with a minimum volume of tissue set at 150 ml. Clusters below this size were ignored in further analysis. The intensity of all pixels within the cluster was set at the maximum intensity within the cluster. Across all subjects, after the saline injection, less than 3% of the voxels in the brain met the strict criteria for activation outlined above. Further, in the group mean activation maps, no clusters of 150 ml or greater were found after the saline injection, indicating a very low probability of a false positive with use of this waveform analysis method.

RESULTS

When measured 2 minutes after administration, nicotine had no significant effect on heart rate or blood pressure. Mean arterial pressure increased only transiently for 10–20 seconds, from a baseline of about 91 mm Hg to a mean peak of about 99.5 mm Hg. Nevertheless, after the nicotine injections the subjects reported experiencing moderate "rush" and "high" feelings that were dose- and time-dependent (mean peak rush scores=2.5, 4.6, and 5.7 out of a possible 10 after the low, medium, and high doses, respectively). Both the rush and the high peaked at 2 minutes after injection and returned to baseline by 5 minutes after. In contrast, scores on pleasantness averaged about 5 at all doses and persisted for 15 minutes. Finally, the participants reported moderately liking the experience (mean peak response rating=4.1, SD=2.1), with no significant effect on feelings of sedation, confusion, or anxiety. Plasma nicotine levels (figure 1) accurately approximated both the behavioral and functional MRI signal time courses. Dose-dependent increases in plasma levels reached maximum values at 2 minutes and rapidly decreased to about two-thirds of peak value within 15 minutes. Baseline nicotine levels were virtually undetectable at less than 10 ng/ml. No prolonged untoward effects were ever reported; all subjects agreed to receive all

TABLE 1. Dose-Response Effects of Intravenous Nicotine Injections on Regional Functional MRI Signals in 16 Subjects[a]

Brain Area	Side Activated After 0.75-mg Dose	After 1.50-mg Dose	After 2.25-mg Dose
Cortex			
Posterior orbital gyrus	Right	Right	
Lateral orbital gyrus	Right		Both
Cingulate cortex	Both	Both	Both
Inferior frontal gyrus	Both	Both	Both
Medial frontal gyrus	Both	Both	Both
Superior frontal gyrus	Left	Both	
Precentral gyrus	Both		
Inferior temporal gyrus	Left	Left	Left
Medial temporal gyrus	Right		Both
Superior temporal gyrus	Both	Left	Left
Insular cortex (posterior)	Left	Left	Left
Insular cortex (anterior)	Both	Both	Left
Postcentral gyrus	Right		Left
Superior parietal cortex		Right	Right
Lingual gyrus	Left	Both	
Angular gyrus	Both	Both	Both
Cuneus	Both	Left	Both
Precuneus	Both		
Medial occipital gyrus	Both	Left	Both
Inferior occipital gyrus		Left	Both
Lateral occipital gyrus			Left
Supramarginal gyrus	Left		Right
Amygdala		Right	Left
Diencephalon			
Pulvinar			Left
Ventral anterior			Both
Medial dorsal nucleus	Left	Right	Both
Dorsal lateral nucleus		Right	
Posterior lateral nucleus	Left		
Anterior nucleus	Right		
Ventral lateral nucleus	Left		Both
Hypothalamus		Left	Both
Basal ganglia			
Putamen		Right	Both
Caudate nucleus	Left		
Nucleus accumbens	Right		Right
Globus pallidus			Right
Superior colliculus			Left
Inferior colliculus			Left

[a]Group data represent the areas that both met the criteria of the waveform recognition algorithm and were significantly different from data obtained after an individual's matched saline injection ($p \leq 0.001$, beta distribution).

nicotine doses, and all returned for subsequent functional MRI scanning.

Regional brain functional MRI signal intensity rapidly increased from baseline levels after nicotine administration, reached a peak response approximately 2.8 minutes after the end of the 1-minute intravenous injection, and returned to one-half of the maximum level approximately 5.6 minutes after drug administration (figure 2). While this response pattern was not the only one seen, it was by far the most dominant and the one used to extract drug-induced localized brain activation from the functional MRI signal. When averaged across all participants, neither percent signal change, time to peak effect, nor time to one-half the maximum effect changed significantly as a function of dose. In contrast, the percentage of voxels activated increased from 3.38% after saline to 7.06%, 11.06%, and 10.90% after the low, medium, and high nicotine doses, respectively ($F=14.35$, $df=3, 45$, $p<0.0001$). The numbers of activated voxels were greater after both the medium and high doses of nicotine compared to saline, and the medium dose effect was also greater than the low dose effect (Scheffé F test, $p \leq 0.05$).

Significant regional activation (table 1) was seen in the insula, anterior and posterior cingulate, frontal lobes (orbital, dorsolateral, and medial frontal), and portions of the temporal and visual occipital cortex. While some visual and frontal regions were activated only after low nicotine doses, perhaps demonstrating rapid response tolerance in these areas to the cumulative dosing paradigm we used, other regions (including temporal, visual, and parietal lobes) became activated only after the higher doses, suggesting a higher threshold for effect in these regions. Finally, a number of limbic subcortical regions were activated (figure 3), including the nucleus accumbens, amygdala, hypothalamus, and several nuclei within the limbic thalamus (e.g., mediodorsal, anterior, and lateroposterior nuclei).

DISCUSSION

In this study, intravenous nicotine strongly activated a distributed system of CNS regions implicated in the control and regulation of many of the behavioral states long attributed to nicotine use. The cingulate and several frontal lobe divisions, including the dorsolateral, orbital, and medial frontal, were among the most prominently activated regions. The frontal lobes—with their rich dopamine innervation—and the cingulate cortex—through its connections with many neocortical association, motor, and sensory regions—have been thought to be involved in the processing of such diverse cognitive states as working memory, attention, motivation, mood, and emotion (17, 18). All of these are known to be modified by nicotine intake (19). In addition, nicotinic receptors are present on both the somatodendritic and axon terminals of locus ceruleus noradrenergic neurons (20), which are known to project to much of the forebrain and hippocampus. These locus ceruleus neurons and their projections are thought to regulate or modulate behavioral arousal and vigilance (21). Taken together with what is known of brain regional structure-function relationships, the functional MRI brain activation pattern in this study is consistent with recurrent reports by cigarette smokers that smoking enhances—whereas smoking abstinence and withdrawal compromise—arousal, mood, vigilance, and attention, among other cognitive processes (19).

Although cigarette smoking has been reported to modify numerous cognitive behaviors, including attention and working memory (8, 19), nicotine's behavioral properties in humans have been difficult to attribute to specific brain regions because of the sometimes subtle and diffuse nature of the drug's effect and the rapid

smoking-withdrawal cycles that make "baseline" behavioral levels difficult to define. This observation may help explain why the cognition-enhancing properties of nicotine have been most convincingly demonstrated in acutely abstinent smokers. It has been more difficult to demonstrate these properties in nonabstinent smokers and in nonsmokers (22), suggesting that some of the reported behavioral effects may reflect withdrawal relief. It has not been demonstrated whether nicotine replacement acts in a "nonspecific" fashion to ameliorate withdrawal-induced dysthymia (alleviation of which might be manifested as a positive effect on cognition) or acts directly on CNS structures primarily involved in cognitive systems. However, in view of the brain regions activated in this study, our data support the hypothesis that direct activation of the frontal and cingulate regions by nicotine is responsible for the drug's primary behavioral and mood-altering effects.

FIGURE 3. Composite Functional MRI Images After Intravenous Injection of 2.25 mg of Nicotine, Averaged Across 16 Subjects, With Individual Brains Normalized Into Talairach Space[a]

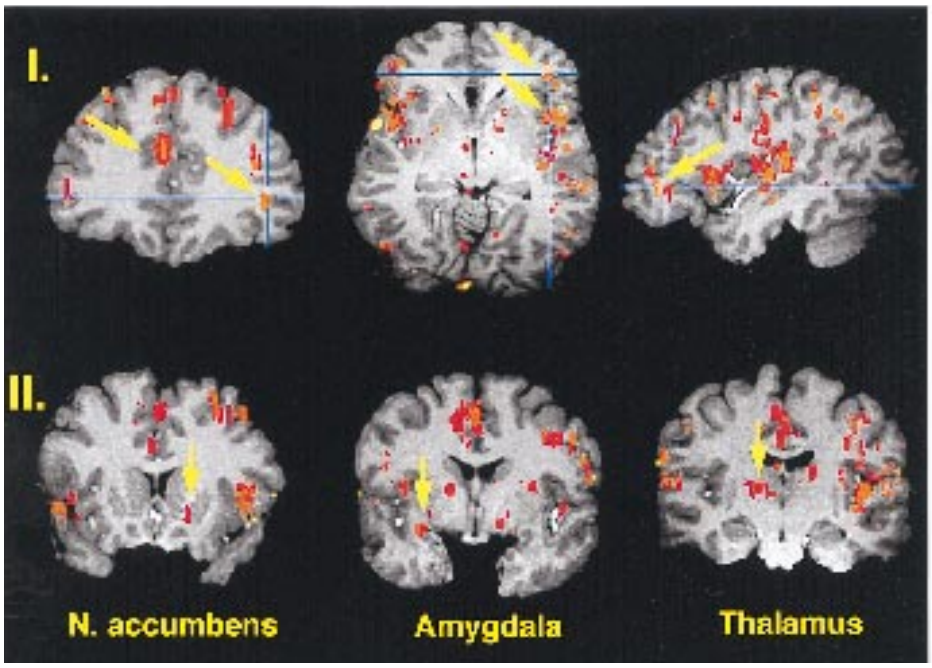

[a](See atlas of Talairach and Tournoux [15]). Areas that met the criteria of the waveform recognition algorithm and were significantly different from saline ($p \leq 0.001$, beta distribution) are indicated in color and superimposed on a single subject's spoiled GRASS anatomical data set. The red-to-yellow color map depicts percent signal change above baseline. Note the relatively constant magnitude of effect across the areas affected by nicotine. Blue crosshairs in part I illustrate equivalent locations in the coronal, sagittal, and axial sections, respectively. Note in the coronal section (part I, left) arrows pointing to the cingulate and lateral orbital gyrus. Additional major areas of activation illustrated include the superior, middle, and inferior frontal gyri. In addition to the indicated lateral orbital gyrus, the axial view (part I, center) illustrates major activation in the insula, colliculus, medial geniculate, hypothalamus, putamen, and globus pallidus, and the sagittal view (part I, right) shows major activation in the insula and transverse temporal gyrus. Notable subcortical limbic regions activated are illustrated in part II and include the nucleus accumbens, amygdala, and thalamus.

Although cigarettes generally produce only a moderate euphorigenic state, human cocaine abusers often identify the effects of intravenous nicotine as similar to and, in many cases, identical to those of intravenous cocaine (4). This observation suggests that the reinforcing and drug-discriminative properties of both drugs probably share common anatomical sites and mechanisms through their ability to ultimately enhance mesocorticolimbic dopamine transmission, albeit through different cellular mechanisms. In this study, among the regions that nicotine activated were the nucleus accumbens, amygdala, limbic thalamus, and frontal lobe cortical regions that have consistently been implicated in the reinforcing properties of both nicotine and cocaine in animal experiments (4, 23–25), suggesting the two drugs' common mechanisms in humans as well. Indeed, the only brain area in the rat that supports direct cocaine self-administration is the medial prefrontal cortex (26), the human homologue of which includes the mediodorsal thalamus terminal fields of the orbitofrontal and medial frontal lobes (27)—regions activated by nicotine in the present study.

To our knowledge, there have been no previously published human studies that have used functional MRI to examine regional patterns of neuronal activity after acute nicotine administration. In two preliminary reports (each with three subjects) (28, 29), Nagata et al. (28) reported increased cerebellar and frontal lobe blood flow after cigarette smoking in a study that used ^{15}O positron emission tomography (PET), while London (29) reported a generalized decrease in glucose uptake after 1.5 mg i.v. of nicotine. Another previous indication of the central sites of nicotine action in the human brain came from the distribution of nicotine-binding sites noted with PET (30). Although receptor binding does not necessarily indicate primary site of action, the present functional activation data agree remarkably well with these human receptor maps. The largest concentrations of [^{11}C]nicotine binding sites are seen in the frontal, cingulate, and insular lobes of the cortex and in the thalamus and basal ganglia. In addition to our observation of significant functional MRI activity in all of these regions, a notable finding from the present study is the significant activation of the vis-

ual cortex. This activation may have been the result of primary nicotinic receptor binding in subcortical visual relay nuclei (e.g., the lateral geniculate) that are known to have high nicotinic receptor concentrations (31, 32) or presynaptic nicotinic binding in the cortex. Nicotinic receptors have also been reported in many thalamic nuclei in rats (33). These nuclei project, in turn, to the temporal lobe auditory and visual occipital cortex and widespread regions of the frontal, cingulate, and parietal cortex. Thus, some of the most activated cortical regions after administration of intravenous nicotine in this study may reflect intense subcortical, thalamic nicotinic receptor activation.

The observation of unilateral regional activation following drug administration was unexpected and deserves mention. Several recent human metabolic mapping studies have reported right dominant activation after administration of cocaine (34) and marijuana (35). While most of the activation sites reported in table 1 were bilateral, many cortical and subcortical sites were activated only unilaterally. Left-right differences in drug effects should be evaluated more closely, since they relate to changes in drug-induced behavioral states.

It is unlikely that the changes in functional MRI signal which we observed were the result of peripheral or central cardiovascular effects. Although nicotine can produce changes in heart rate and blood pressure (3), which by themselves can indirectly alter global cerebral blood flow, no significant cardiovascular changes were seen in the present experiment, which involved well-experienced, nicotine-tolerant subjects. Cerebral blood flow may also be influenced by changes in respiratory-dependent P_{CO_2} following nicotinic ganglionic activation. However, such peripheral modulation would likely produce homogeneous alterations in blood flow and blood-oxygen-level-dependent signal rather than the more distributed, heterogeneous pattern of activation we observed. In addition, the blood-oxygen-level-dependent weighted pulse sequence and long interscan time used in this study are heavily weighted to reflect changes in local oxygenation more than blood flow (36). Changes in regional brain metabolism (oxygen extraction and glucose utilization) are more uniquely linked to neuronal activity than changes in cerebral blood flow, which may potentially reflect more generalized vascular alterations independent of regional brain activity, as in CO_2-induced vasodilation (37).

Taken together, these data suggest that the observed functional MRI signal changes reflect alterations in neuronal activity secondary to CNS nicotinic receptor activation. The data from this study are the first to describe the CNS regions acted upon by acute nicotine administration in humans, are neuroanatomically consistent with the mood-elevating and anxiolytic effects often ascribed to cigarette smoking (19), and support our hypothesis that the observed cortical activation underlies many of the behavioral properties of the drug. By revealing the regional activation and, importantly, the time course of nicotine's action in the human brain (a feature that functional MRI is uniquely qualified to examine), these data support the role of nicotine in the behavioral effects observed during cigarette smoking. Notably, the real-time functional MRI signal in this study peaked at approximately 2.8 minutes after drug administration and is consistent with the peak plasma nicotine concentration observed at approximately 2 minutes and the reported peak behavioral effects.

Finally, it should be noted that other nicotine-induced functional MRI waveforms were also occasionally observed but not analyzed for this report. For example, some waveforms increased at an appropriate postinjection time but did not return to baseline during the a priori allotted time window for analysis. Whether this response pattern reflects a neuronally induced, alternative drug effect (e.g., prolonged activation) is currently under investigation. For example, it might be posited that multiple brain timing circuits are engaged by cigarette smoking, leading to behaviors with different time constants, i.e., variable interpuff intervals (in tens of seconds) and intercigarette intervals (tens to hundreds of minutes). Only real-time measurements such as functional MRI have the potential to identify brain regions responsible for distinct portions of this complex behavior. It may now be possible to separate the CNS sites responsible for nicotine's reinforcing properties from the drug's other pharmacological effects. This would permit testing hypotheses about the commonality of mechanisms in abused drugs as well as serve as a powerful "bioassay" in the development of agents to manage and treat nicotine abuse.

REFERENCES

1. Jaffe J: Tobacco smoking and nicotine dependence, in Nicotine Psychopharmacology: Molecular, Cellular and Behavioral Aspects. Edited by Wonnacott S, Russell MAH, Stolerman IP. New York, Oxford Press, 1990, pp 1–37
2. Centers for Disease Control: Smoking cessation during the previous year among adults—United States, 1990 and 1991. MMWR Morb Mortal Wkly Rep 1993; 42:504–507
3. Henningfield JE, Miyasato K, Jasinski DR: Abuse liability and pharmacodynamic characteristics of intravenous and inhaled nicotine. J Pharmacol Exp Ther 1985; 234:1–12
4. Henningfield JE, Miyasato K, Jasinski DR: Cigarette smokers self-administer intravenous nicotine. Pharmacol Biochem Behav 1983; 19:887–890
5. Stolerman IP, Jarvis MJ: The scientific case that nicotine is addictive. Psychopharmacology (Berl) 1995; 117:2–10
6. Corrigall WA, Franklin KBJ, Coen KM, Clarke PBS: The mesolimbic dopaminergic system is implicated in the reinforcing effects of nicotine. Psychopharmacology (Berl) 1992; 107:285–289
7. Corrigall WA, Coen KM: Selective dopamine antagonists reduce nicotine self-administration. Psychopharmacology (Berl) 1991; 104:171–176
8. Aceto MD, Martin BM: Central actions of nicotine. Med Res Rev 1982; 2:43–62
9. London ED, Connolly RJ, Szikszay M, Wamsley JK, Dam M: Effects of nicotine on local cerebral glucose utilization in the rat. J Neurosci 1988; 8:3920–3928
10. Clarke PBS, Pert A: Autoradiographic evidence for nicotine receptors on nigrostriatal and mesolimbic dopaminergic neurons. Brain Res 1985; 348:355–358
11. Grunwald F, Schrock H, Kuschinsky W: The influence of nicotine on local cerebral blood flow in rats. Neurosci Lett 1991; 124:108–110

12. Oldfield RC: The assessment and analysis of handedness: the Edinburgh Inventory. Neuropsychologia 1971; 9:97–113
13. Feyerabend C, Russell MAH: A rapid gas-liquid chromatographic method for the determination of cotinine and nicotine in biological fluids. J Pharm Pharmacol 1990; 42:450–452
14. Wong EC, Boskamp E, Hyde JS: A volume optimized quadrature elliptical endcap birdcage brain coil. Berlin, 11th Annual Scientific Meeting, Society for Magnetic Resonance Medicine, 1992, 4015
15. Talairach J, Tournoux P: Co-Planar Stereotaxic Atlas of the Human Brain. New York, Thieme Medical, 1988
16. Cox RW: AFNI: software for analysis and visualization of functional magnetic resonance neuroimages. Comput Biomed Res 1996; 29:162–173
17. Devinsky O, Luciano D: The contributions of cingulate cortex to human behavior, in Neurobiology of Cingulate Cortex and Limbic Thalamus: A Comprehensive Handbook. Edited by Vogt BA, Gabriel M. Boston, Birkhauser, 1993, pp 527–556
18. Sawaguchi T, Goldman-Rakic PJ: The role of D1-dopamine receptor in working memory: local injections of dopamine antagonists into the prefrontal cortex of rhesus monkeys performing an oculomotor delayed-response task. J Neurophysiol 1994; 71:515–528
19. Warburton DM: Psychopharmacological aspects of nicotine, in Nicotine Psychopharmacology: Molecular, Cellular and Behavioral Aspects. Edited by Wonnacott S, Russell MAH, Stolerman IP. New York, Oxford University Press, 1990, pp 77–111
20. Mitchell SN: Role of the locus coeruleus in the noradrenergic response to a systemic administration of nicotine. Neuropharmacology 1993; 32:937–949
21. Aston-Jones G, Rajkovski J, Kubiak P, Alexinsky T: Locus coeruleus neurons in monkey are selectively activated by attended cues in a vigilance task. J Neurosci 1994; 14:4467–4480
22. Heishman SJ, Taylor RC, Henningfield JE: Nicotine and smoking: a review of effects on human performance. Exp Clin Psychopharmacol 1994; 2:345–395
23. Pich EM, Pagliusi SR, Tessari M, Talabot-Ayer D, Hooft van Huijsduijnen R, Chiamulera C: Common neural substrates for the addictive properties of nicotine and cocaine. Science 1997; 275:83–86
24. Wise RA, Rompre PR: Brain dopamine and reward. Ann Rev Psychol 1989; 40:191–225
25. Porrino LJ: Metabolic mapping of the effects of cocaine in the brain, in Cocaine: Pharmacology, Physiology and Clinical Strategies. Edited by Lakoski JM, Galloway MP, White FJ. Boca Raton, CRC Press, 1992, pp 35–46
26. Goeders NE, Smith JE: Cortical dopaminergic involvement in cocaine reinforcement. Science 1983; 221:773–775
27. Groenewegen HJ: Organization of the afferent connections of the mediodorsal thalamic nucleus in the rat, related to the medio-dorsal-prefrontal topography. Neuroscience 1988; 24: 379–431
28. Nagata K, Shinohara T, Kanno I, Hatazawa J, Domino EF: Effects of tobacco cigarette smoking on cerebral blood flow in normal adults, in Brain Imaging of Nicotine and Tobacco Smoking. Edited by Domino EF. Ann Arbor, Mich, NPP Books, 1995, pp 95–108
29. London ED: Mapping the cerebral metabolic response to nicotine. Ibid, pp 153–166
30. Nyback H, Nordberg A, Langstrom B, Halldin C, Hartvig P, Halin A, Swahn CG, Sedvall G: Attempts to visualize nicotinic receptors in the brain of monkey and man by positron emission tomography. Prog Brain Res 1989; 79:313–319
31. Prusky GT, Shaw C, Cyander MS: Nicotine receptors are located on lateral geniculate nucleus terminals in cat visual cortex. Brain Res 1987; 412:131–138
32. Clarke PBS, Pert CB, Pert A: Autoradiographic distribution of nicotine receptors in rat brain. Brain Res 1984; 323:390–395
33. Clarke PBS, Schwartz RD, Paul SM, Pert CB, Pert A: Nicotinic binding in rat brain: autoradiographic comparison of [3H]acetylcholine, [3H]nicotine, and [125I]-alpha-bungarotoxin. J Neurosci 1985; 5:1307–1315
34. Breiter HC, Gollub RL, Weiskoff RM, Kennedy DN, Makris N, Berke JD, Goodman JM, Kantor HL, Gastfriend DR, Riorden JP, Matthew RT, Rosen BR, Hyman SE: Acute effects of cocaine on human brain activity and emotion. Neuron 1997; 19: 591–611
35. Matthew RJ, Wilson WH, Coleman E, Turkington TG, DeGrado TR: Marijuana intoxication and brain activation in marijuana smokers. Life Sci 1997; 60:2075–2089
36. Ogawa S, Tank DW, Menon R, Ellerman JM, Kim SG, Merkle N, Ugurbil K: Intrinsic signal changes accompanying sensory stimulation: functional brain mapping with magnetic resonance imaging. Proc Natl Acad Sci USA 1992; 89:5951–5955
37. Sokoloff L: Metabolic Probes of Central Nervous System Activity in Experimental Animals and Man. Sunderland, Mass, Sinauer Associates, 1984